International Journal of General Medicine

Dovepress
Taylor & Francis Group

Open Access Full Text Article

ORIGINAL RESEARCH

Multiomics-Based Deep Learning Prediction of Prognosis and Therapeutic Response in Patients With Extensive-Stage Small Cell Lung Cancer Receiving Chemoimmunotherapy: A Retrospective Cohort Study

Fang Nie*, Xiufeng Pei*, Jiale Du, Wanting Shi, Jianying Wang, Lu Feng, Yonggang Liu

Department of Thoracic Oncology, Baotou Cancer Hospital, Baotou, Inner Mongolia, 014000, People's Republic of China

*These authors contributed equally to this work

Correspondence: Yonggang Liu, Email zlnkldf8000@sina.com

Objective: This study aimed to develop a clinical early warning prediction model to evaluate the prognosis and response to chemoimmunotherapy in patients with extensive-stage small cell lung cancer (ES-SCLC), thereby guiding clinical decision-making.

Methods: A retrospective analysis was conducted on the clinical data and radiomics parameters of 309 patients with ES-SCLC hospitalized at Baotou Cancer Hospital from February 2020 to September 2024. Patients were divided into reactive and non-reactive groups based on their response to chemoimmunotherapy.Machine learning algorithms (including random forests, decision trees, artificial neural networks, and generalized linear regression) were used to predict the combined treatment response. The model's predictive ability was evaluated using the receiver operating characteristic (ROC) curve and clinical decision curve analysis(DCA). The prognostic evaluation of patients receiving combination therapy was based on the COX regression model, with predictive performance assessed through nomogram visualization and calibration curves.

Results: Out of 309 patients with ES-SCLC, 248 (80.26%) responded to combination therapy. Logistic regression and Least absolute shrinkage and selection operator (LASSO) regression analyses identified Energy, sum of squares(SOS), mean sum(MES), sum variance(SUV), sum entropy(SUE), difference variance(DIV), and pathomics score as independent risk factors for treatment response. The area under the ROC curve for predicting treatment response using machine learning were 0.764 (95% confidence interval [CI]: 0.707~0.821) and 0.901 (95% CI: 0.846~0.956) in the training and validation sets. The C-index of the radiomics and pathomics prognostic nomogram model based on the COX prognostic model was 0.766 and 0.812 in those sets, respectively.

Conclusion: We developed prediction model based on multi-omics demonstrated satisfactory performance in predicting chemoimmunotherapy response in patients with ES-SCLC. The random forest prediction model, in particular, provides accurate response and prognostic risk assessments, thereby assisting clinical decision-making.

Keywords: extensive-stage small cell lung cancer, immune combination therapy, therapeutic response, radiomics, machine learning, prediction model

Introduction

Small cell lung cancer (SCLC) is an aggressive neuroendocrine malignancy characterized by rapid growth and early widespread metastasis, accounting for 13% to 15% of all lung cancer cases.[1,2] Approximately two-thirds of initially diagnosed SCLC cases are at the extensive stage.[3,4] For the past 30 years, the standard first-line treatment for extensive-stage SCLC (ES-SCLC) has been a combination of etoposide and platinum; however, its overall efficacy is limited, with a median survival of only 8–13 months.[5,6] Recently, immune checkpoint inhibitors, particularly antibodies targeting

Received: 14 November 2024
Accepted: 4 February 2025
Published: 24 February 2025

programmed death receptor-1 (PD-1) and programmed death receptor ligand-1 (PD-L1), have shown promise in improving the prognosis of ES-SCLC. These treatments are emerging as potential new clinical approaches.[7] The results of an IMpower133 study demonstrated that the combination of atezolizumab and chemotherapy reduced the risk of death in patients with ES-SCLC by 30% and provided a 2-month overall survival benefit.[8] The CASPIAN study further confirmed that immunotherapy combined with chemotherapy as a first-line treatment can prolong the overall survival of these patients.[9] However, the benefits of immunotherapy are not universal among patients with ES-SCLC, especially the overall improvement in efficacy is limited, with overall survival extended by only 2–4 months.[10,11] Collectively, the treatment regimen of immunotherapy combined with chemotherapy does not benefit all patients with ES-SCLC, even patients with similar conditions may have different responses and prognoses. Therefore, it is crucial to identify this treatment's potential beneficiaries and to explore new immunotherapy regimens that could enhance efficacy. Increasing researchers have attempted to identify the potential benefits of immunotherapy combined with chemotherapy by examining tumor tissue PD-L1 expression and tumor mutation burden.[12,13] However, due to tumor heterogeneity and limitations in PD-L1 detection methods, these potential predictive biomarkers have not yet been widely applied in clinical practice.

Recently, with the increased use of radiomics and artificial intelligence in medicine, combining non-invasive radiomics feature extraction with artificial intelligence multimodal algorithms to construct machine learning prediction models has shown promise for improving diagnostic and treatment efficiency.[14] For example, Zhao et al used a comprehensive clinical and radiomics model to predict the treatment outcomes of ES-SCLC patients receiving chemoimmunotherapy, providing a convenient and low-cost prognostic model for patient management decision-making.[15] Additionally, the field of pathology is rapidly transitioning from semi quantitative and empirical science to the discipline of big data, and mathematical modeling through systematic pathology methods is an ideal medium for extracting important information from these large, multi parameter, and hierarchical datasets.[16] Systemic pathology can also predict dynamic responses to disease progression or treatment plans from static tissue samples, especially by combining big data with systemic medicine, providing personalized clinical practice for prognosis and predictive patient care.[16,17] However, the integration of multiple omics (ie pathology and radiomics) to evaluate the efficacy of ES-SCLC immunotherapy combined with chemotherapy response has not been fully revealed.

Encouraged by these advancements, this study investigated multiomics biomarkers to predict the therapeutic efficacy of immunotherapy combined with chemotherapy and prognosis in ES-SCLC. The goal was to obtain reliable predictive biomarkers to guide precise chemoimmunotherapy in patients with ES-SCLC.

Materials and Methods

Study Population

Data from 309 patients with ES-SCLC were retrospectively collected from those who received immunotherapy combined with chemotherapy at the front line of Baotou Cancer Hospital from February 2020 to September 2024. Inclusion criteria: 1) Patients confirmed by pathology to have SCLC and classified as ES according to the American Veterans Administration Lung Study Group (VALSG) staging system; 2) Patients who received immunotherapy combined with chemotherapy as first-line treatment for ES-SCLC; 3) Those with an Eastern Oncology Collaboration Group performance status score of 0–2; 4) Those with complete and accessible clinical pathological information and radiomics features. Exclusion criteria: 1) Patients with multiple primary tumors in different locations; 2) Patients with concomitant blood diseases or autoimmune diseases; 3) Patients with severe infectious diseases or mental illness; 4) Patients for whom lung radiomics features cannot be accurately obtained or who have missing imaging data. This study strictly adhered to the Helsinki Declaration, retrospectively collected patient medical records that met the inclusion criteria, encrypted all personal information, and received approval from the Baotou Cancer Hospital Ethics Committee. Patient informed consent was waived. The patient inclusion and prediction model construction process is depicted in Figure 1.

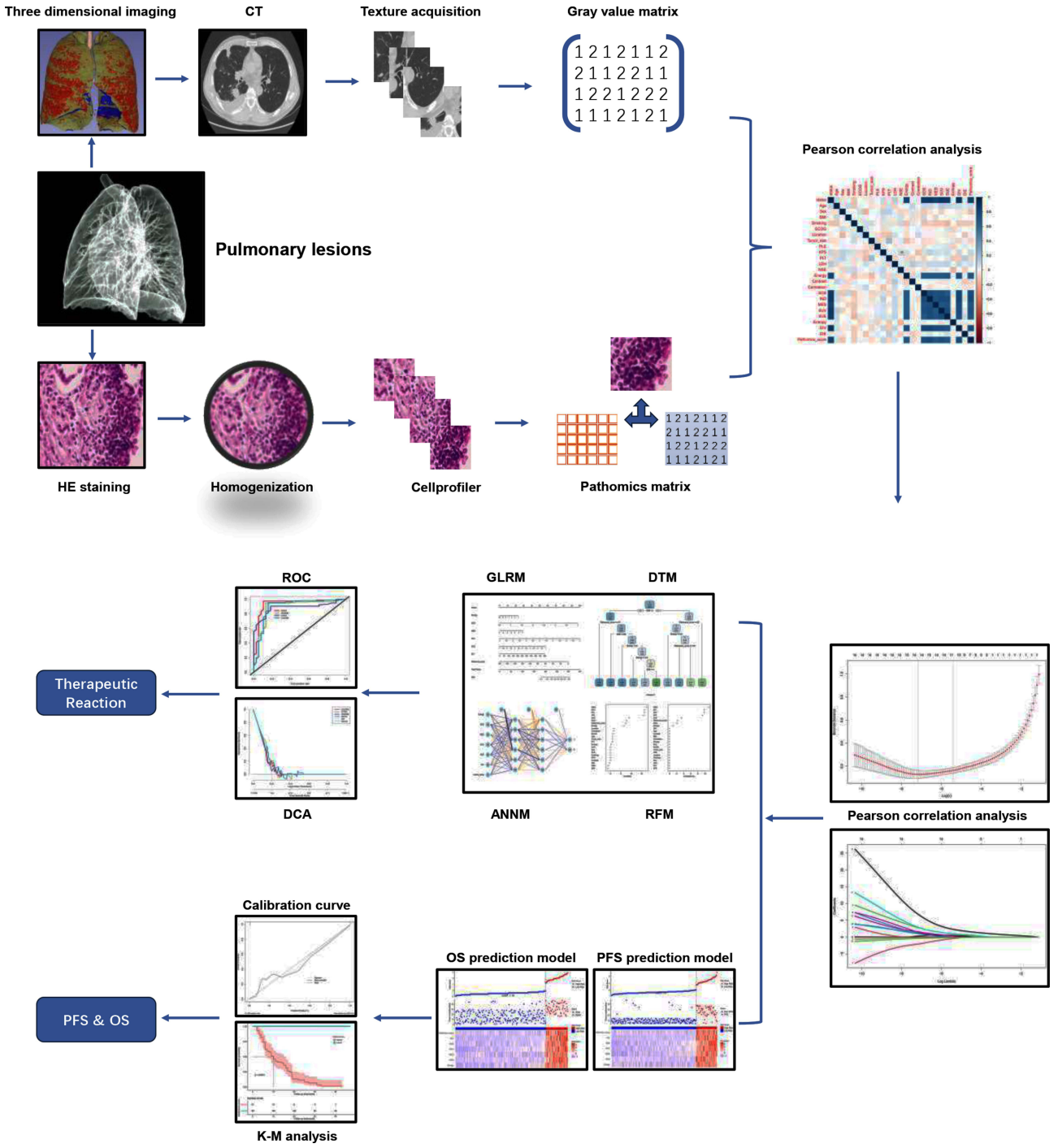

Figure 1 Flow chart for obtaining radiological and pathological features and constructing predictive models.

Treatment Plan and Efficacy Evaluation

All patients with ES-SCLC received treatment with anti-PD-L1. The specific treatment plan was as follows: 1) Four cycles of induction treatment every 21 days: patients received atezolizumab 1200mg and carboplatin (area under the curve [AUC]=5) on the first day of each cycle; etoposide 100mg/m^2 on the first to third days of each cycle; 2) Alternatively, durvalumab 1500mg on the first day of each cycle, cisplatin 75–80mg/m^2, and etoposide 80–100mg/m^2. After induction, patients enter the maintenance period, receiving atezolizumab 1200mg/21 days or durvalumab 1500mg/21 days until severe toxic reactions or disease progression occur. We evaluate the optimal objective response of ES-

https://doi.org/10.2147/IJGM.S506485

SCLC patients after treatment based on the Response Evaluation Criteria in Solid Tumors V.1.1, which measures changes in tumor diameter to reflect changes in tumor volume, including complete remission(CR), partial remission(PR), disease stability(SD), and disease progression(PD).[18] We use objective remission rate as an evaluation indicator for effective treatment response, ie DCR= (CR+PR)/total cases × 100%. The overall survival(OS) period is defined as the time from the start of treatment to death from any cause, and progression free survival(PFS) refers to the time from the patient's initiation of treatment until the first tumor progression or death. The last follow-up period ends on October 30, 2024.

Radiomics Feature Extraction

All chest CT scans with contrast were performed using a multi row CT scanner: Philips Healthcare (Brilliance 16, Huachen iCT, IQON Spectral CT, Siemens Healthineers (Somatom Sensation 64, Somatom Deflation), General Electric Healthcare (GE Revolution, Discovery CT 750 hD), Toshiba Medical Systems (Aquilion One). CT scan parameters were set: tube voltage: 100–140kV, tube current: 149–752mA, and CT scan layer thickness: 1.0–5.0mm. Tumor contours were delineated layer by layer in the baseline CT scan images, extracting features including six tumor morphological features, four tumor texture features, two tumor boundary features, and 15 tumor intensity features. For texture depth analysis, the spatial resolution of CT images was isotropically resampled to $1.0mm^3$, and a quantization scheme was applied with a fixed frame width of 5 hounsfield units to the image pixel values. A 3D slicer was used to analyze the adjusted CT image co-occurrence grayscale matrix to extract non-redundant radiomics features.

Pathological Omics Feature Extraction

Tumor lesion biopsy is mainly performed under CT guidance. We use a step-by-step needle insertion method. Based on CT positioning, we first puncture the needle outside the parietal pleura for local anesthesia, and then place the needle inside the lung tissue for scanning confirmation. If the needle insertion path is correct, the puncture needle can be directly inserted into the lesion. Firstly, soak the biopsy tissue in formalin with a concentration of 10% for 4 hours, and then embed it in immunohistochemical paraffin. Subsequently, the wax blocks were sliced at intervals of 4 μ m and stained with hematoxylin and eosin for pathological evaluation. Pathologists use a digital slide scanner (KFBio KF-PRO-020) to scan all pre-treatment tissue pathology sections at a 40x scanning magnification to obtain digital pathology sections of the patient. In the digital slicing manager, the sample was magnified by 10 times, and the pathologist selected a representative sample area and obtained a 512×512 pixel screenshot, which was then confirmed by another pathologist with 3 and 8 years of pathological diagnosis experience, respectively. If two pathologists have different opinions, they will discuss with the third pathologist to make a decision. The process of extracting pathological features is shown in Figure 1.

Prediction Model Construction

To identify the optimal radiomics features before constructing the prediction model, the Least Absolute Shrinkage and Selection Operator (LASSO) method is used to select the optimal variable of risk factors to predict the response of ES-SCLC to treatment, that is, the outcome is the presence or absence of response. LASSO regression effectively reduces some feature coefficients to zero in the regression model. We selected the LASSO regression model with non-zero features as the variable.[19] Recent advancements in machine learning algorithms led to incorporating candidate prediction parameters into algorithms such as random forests, decision trees, artificial neural networks, and generalized linear models.[20–22] The prediction performance and robustness were evaluated by calculating the area under the receiver operating characteristic (ROC) curve, analyzing the decision curve, and performing repeated iterations for each prediction model.

Statistical Analysis

All data analysis and visualization were conducted using R software (version 4.2.3). Independent sample *t*-tests or Mann–Whitney *U*-tests were used for continuous variables, and chi-square tests or Fisher's exact tests were used for categorical variables. All machine learning algorithms for prediction models were implemented using the R software package (such as *rms, glmr*, etc.) in the training set cohort. Decision analysis was performed by quantifying the net benefits under

different threshold probabilities across the entire dataset to assess the clinical practicality and net benefits of the radiomics prediction model. All tests are bilateral, with statistical significance set at P<0.05.

Results

Study Population and Treatment Outcomes

A comprehensive imaging evaluation of 309 patients with ES-SCLC was conducted after treatment completion. Among these, 100 cases (32.36%) achieved complete response (CR), 147 achieved partial response (PR) (47.57%), 10 patients had stable disease (SD) (3.24%), and 52 patients had progressive disease (PD) (16.83%). The overall response rate (ORR) and disease control rate (DCR) were 79.94% and 83.17%, respectively. As of the last follow-up, the median progression-free survival time was 14.1 months (95% CI: 4.13–24.59). Comparative analysis of clinical baseline data and radiomics and pathomics characteristics between the patients of the response and non-response groups is shown in Table 1 and Supplementary Table 1, highlighting radiomics characteristics, such as Energy, sum of squares(SOS), inverse difference(IND), mean sum(MES), sum variance(SUV), sum entropy(SUE), and difference variance(DIV) (all P<0.05).

Extraction of Response Prediction Radiomics Feature

As shown in Figure 2, the LASSO regression was chosen to select the optimal radiomics features. The final grayscale region size matrix and grayscale co-occurrence matrix retained seven optimal radiomics features predictive of response to immunotherapy combined with chemotherapy: Energy, SOS, MES, SUV, SUE, DIV, and pathomics score. Moreover, univariate and multivariate logistic regression analysis indicated that these features are independent risk factors for response to immunotherapy combined with chemotherapy (Table 2 and Supplementary Table 2). These results consistently demonstrate the potential for predicting targeted therapy response based on radiomics feature parameter comparison.

Construction of the Radiomics-Based ML Prediction Model

Through LASSO regression and random forest recursive feature elimination filtering, four machine learning prediction models were established: random forest model, decision tree model, artificial neural network model, and generalized linear model (Figure 3 and Supplementary Figure 1). By performing cross-validation and analyzing the area under the ROC curve and decision curve, the predictive performances of these models were compared. The random forest model, constructed using Energy, SOS, MES, SUV, SUE, DIV, and pathomics score exhibited the best predictive performance, with AUC of 0.899 and 0.901 in the training and validation sets, respectively. The area under the ROC curve for the decision tree, artificial neural network, and generalized linear models is higher than 0.75 (Table 3 and Figure 4).

Performance of the Integrated Model for Response Prediction

The decision curve analysis (DCA) indicates that within the risk threshold range of 10% to 90%, the random forest model predicts better clinical net benefits for the response to immunotherapy combined with chemotherapy response than other prediction models (Figure 4). The COX regression results suggest that radiomics parameters and pathomics are independent risk factors for the progression-free survival prognosis of ES-SCLC after receiving immunotherapy combined with chemotherapy (Supplementary Tables 3 and 4). Moreover, the predictive performance of the prognostic evaluation prediction model, obtained through nomogram visualization, is robust, with C-index values of 0.766 and 0.812 in the training and validation sets, respectively (Figures 5 and 6). Furthermore, SHAP results show that Energy, SOS, MES, SUV, SUE, DIV, and pathomics score are associated with higher SHAP values, indicating a more significant predictive value for the prognosis to immunotherapy combined with chemotherapy (Supplementary Table 5). In summary, the random forest model best predicted the response risk to immunotherapy combined with chemotherapy. The prediction model based on radiomics parameters can provide a reference for treatment and prognosis decision-making in ES-SCLC.

https://doi.org/10.2147/IJGM.S506485

Table 1 Baseline and Demographic Comparison of Study Population

Variables	Training Cohort			p-value	Testing Cohort			p-value
	Overall (N=216)	Non-Response (N=45)	Response (N=171)		Overall (N=93)	Non-Response (N=16)	Response (N=77)	
Age (median [IQR])	45.50 [34.75, 56.00]	50.00 [37.00, 62.00]	44.00 [33.50, 54.50]	0.027	47.00 [34.00, 60.00]	45.00 [35.75, 63.00]	48.00 [34.00, 60.00]	0.919
Sex (%)								
Male	126 (58.3)	29 (64.4)	97 (56.7)	0.444	43 (46.2)	7 (43.8)	36 (46.8)	1
Female	90 (41.7)	16 (35.6)	74 (43.3)		50 (53.8)	9 (56.2)	41 (53.2)	
BMI (median [IQR])	25.00 [21.92, 28.33]	25.00 [22.10, 29.20]	25.00 [21.70, 28.30]	0.84	24.00 [21.10, 28.20]	23.55 [20.70, 27.95]	24.10 [21.30, 28.60]	0.316
Smoking (%)								
Yes	107 (49.5)	30 (66.7)	77 (45.0)	0.016	48 (51.6)	8 (50.0)	40 (51.9)	1
No	109 (50.5)	15 (33.3)	94 (55.0)		45 (48.4)	8 (50.0)	37 (48.1)	
ECOG (%)								
0	71 (32.9)	12 (26.7)	59 (34.5)	0.529	36 (38.7)	7 (43.8)	29 (37.7)	0.37
1	69 (31.9)	17 (37.8)	52 (30.4)		26 (28.0)	6 (37.5)	20 (26.0)	
2	76 (35.2)	16 (35.6)	60 (35.1)		31 (33.3)	3 (18.8)	28 (36.4)	
Location (%)								
Left	110 (50.9)	23 (51.1)	87 (50.9)	1	39 (41.9)	8 (50.0)	31 (40.3)	0.66
Right	106 (49.1)	22 (48.9)	84 (49.1)		54 (58.1)	8 (50.0)	46 (59.7)	
Tumor_size (%),cm								
≥4	94 (43.5)	23 (51.1)	71 (41.5)	0.324	54 (58.1)	9 (56.2)	45 (58.4)	1
<4	122 (56.5)	22 (48.9)	100 (58.5)		39 (41.9)	7 (43.8)	32 (41.6)	
PLE (%)								
Yes	107 (49.5)	21 (46.7)	86 (50.3)	0.791	43 (46.2)	8 (50.0)	35 (45.5)	0.955
No	109 (50.5)	24 (53.3)	85 (49.7)		50 (53.8)	8 (50.0)	42 (54.5)	
KPS (%)								
≥80	96 (44.4)	20 (44.4)	76 (44.4)	1	37 (39.8)	1 (6.2)	36 (46.8)	0.006
<80	120 (55.6)	25 (55.6)	95 (55.6)		56 (60.2)	15 (93.8)	41 (53.2)	
PLT (%),*109/L								
≥350	96 (44.4)	23 (51.1)	73 (42.7)	0.399	54 (58.1)	10 (62.5)	44 (57.1)	0.907
<350	120 (55.6)	22 (48.9)	98 (57.3)		39 (41.9)	6 (37.5)	33 (42.9)	
LDH (%),IU/L								
≥250	108 (50.0)	18 (40.0)	90 (52.6)	0.18	46 (49.5)	5 (31.2)	41 (53.2)	0.185
<250	108 (50.0)	27 (60.0)	81 (47.4)		47 (50.5)	11 (68.8)	36 (46.8)	
NSE (%),ng/mL								
≥15	129 (59.7)	31 (68.9)	98 (57.3)	0.216	44 (47.3)	5 (31.2)	39 (50.6)	0.255
<15	87 (40.3)	14 (31.1)	73 (42.7)		49 (52.7)	11 (68.8)	38 (49.4)	
Energy (median [IQR])	3.80 [2.51, 5.96]	10.06 [7.08, 11.06]	3.20 [2.32, 4.66]	<0.001	4.29 [2.64, 5.81]	8.50 [6.73, 10.89]	3.66 [2.44, 4.78]	<0.001
Contrast (median [IQR])	270.00 [248.00, 298.00]	270.00 [251.00, 304.00]	271.00 [247.50, 295.00]	0.846	273.00 [254.00, 308.00]	275.50 [245.50, 305.00]	273.00 [260.00, 310.00]	0.498
Correlation (median [IQR])	16.01 [12.08, 19.67]	15.63 [13.43, 17.46]	16.19 [11.93, 19.87]	0.472	15.70 [11.20, 19.57]	15.38 [14.52, 16.19]	15.81 [10.99, 19.59]	0.752
SOS (median [IQR])	0.93 [0.72, 1.07]	2.68 [1.92, 3.13]	0.86 [0.70, 1.00]	<0.001	0.89 [0.71, 1.06]	2.20 [1.77, 3.13]	0.83 [0.71, 0.98]	<0.001

IND (median [IQR])	1.54 [1.17, 1.88]	3.56 [2.80, 4.13]	1.39 [1.12, 1.65]	<0.001	1.42 [1.13, 1.87]	3.28 [2.86, 3.93]	1.33 [1.11, 1.66]	<0.001
MES (median [IQR])	2.67 [1.93, 3.40]	4.98 [4.30, 6.23]	2.29 [1.71, 2.94]	<0.001	2.63 [2.00, 3.33]	4.79 [4.24, 5.32]	2.48 [1.84, 2.97]	<0.001
SUV (median [IQR])	2.20 [1.70, 2.62]	4.74 [4.22, 5.73]	2.03 [1.63, 2.33]	<0.001	1.99 [1.56, 2.61]	4.53 [3.65, 5.16]	1.79 [1.52, 2.21]	<0.001
SUE (median [IQR])	2.10 [1.69, 2.70]	4.75 [4.03, 5.90]	1.90 [1.60, 2.36]	<0.001	2.18 [1.73, 2.59]	4.45 [3.96, 5.84]	2.03 [1.60, 2.40]	<0.001
Entropy (median [IQR])	2.30 [1.72, 2.91]	2.25 [1.75, 2.66]	2.31 [1.71, 2.96]	0.796	2.27 [1.74, 3.04]	2.49 [2.06, 3.09]	2.11 [1.69, 3.03]	0.321
DIV (median [IQR])	88.00 [70.00, 114.00]	308.00 [233.00, 409.00]	81.00 [64.50, 94.00]	<0.001	88.00 [63.00, 110.00]	341.50 [224.50, 399.25]	77.00 [62.00, 97.00]	<0.001
DIE (median [IQR])	251.00 [205.25, 286.25]	259.00 [220.00, 293.00]	246.00 [202.00, 285.00]	0.313	220.00 [180.00, 286.00]	222.00 [173.75, 273.25]	218.00 [186.00, 286.00]	0.795
Pathomics_score (median [IQR])	27.00 [16.00, 39.25]	109.00 [71.00, 151.00]	22.00 [14.00, 31.50]	<0.001	22.00 [13.00, 35.00]	107.00 [81.75, 151.75]	20.00 [11.00, 29.00]	<0.001

Abbreviations: IQR, inter-quartile range; BMI, Body mass index; ECOG, Eastern cooperative oncology group; PLE, Pleural effusion; KPS, Karnofsky; PLT, Platelet count; LDH, Lactate dehydrogenase; NSE, Neuro-specific enolase; SOS, sum of squares; IND, inverse difference; MES, mean sum; SUV, sum variance; SUE, sum entropy; DIV, difference variance; DIE, difference entropy.

https://doi.org/10.2147/IJGM.S506485

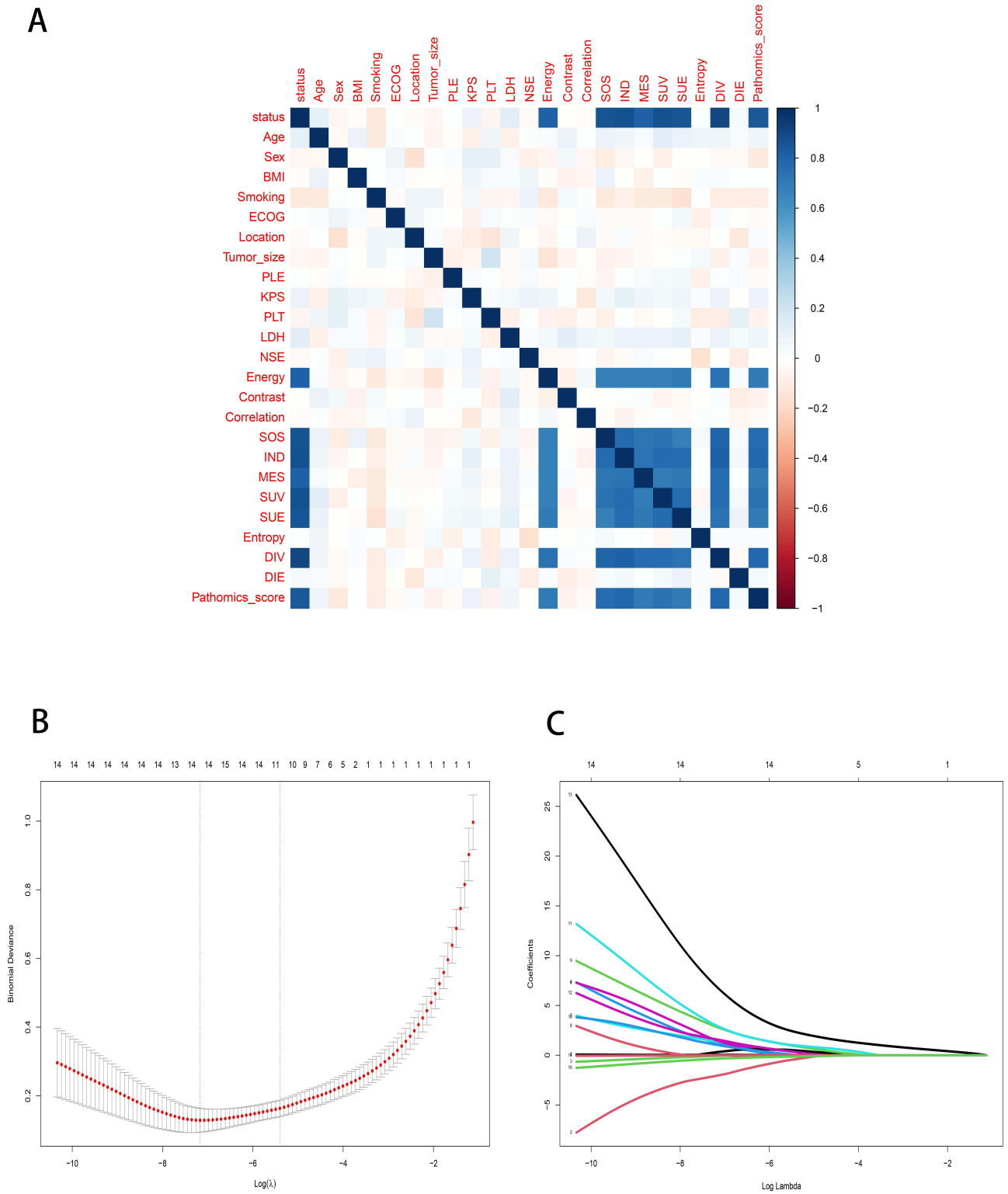

Figure 2 Selection of candidate variables for predictive models. (**A**) The correlation analysis between Pearson correlation coefficient candidate variables and outcomes, where "outcome" refers to treatment response; (**B**) The optimal parameter (λ) selection for the LASSO model was obtained through 10 fold cross validation. Draw a dashed vertical line at the optimal value based on the minimum standard and one standard error of the minimum standard; (**C**) The LASSO coefficient displays all candidate predictive features. A coefficient contour plot was plotted based on the logarithmic (λ) sequence.

Table 2 Multivariate Logistic Regression Analysis of Chemoimmunotherapy Response Based on Radiomics and Pathomics

Variables	Univariate Analysis			p-value	Multivariate Analysis			p-value
	OR	95% CI Lower	95% CI Upper		OR	95% CI Lower	95% CI Upper	
Energy	1.36	0.21	3.18	<0.01	1.52	0.33	3.04	<0.01
SOS	2.25	0.86	5.26	<0.01	2.31	0.79	4.98	<0.01
MES	3.54	1.02	5.33	<0.01	3.49	0.99	5.12	<0.01
SUV	2.84	0.06	3.17	<0.01	2.98	0.23	3.26	<0.01
SUE	2.09	0.56	3.54	<0.01	2.11	0.61	3.88	<0.01
DIV	1.88	0.48	3.01	<0.01	1.92	0.55	3.45	<0.01
Pathomics score	3.07	1.02	7.45	<0.01	2.99	0.89	5.26	<0.01

Abbreviations: OR, Odds ratio; 95% CI, 95% confidence interval.

Discussion

Although immunotherapy has been hailed as the first-line treatment for ES-SCLC, it cannot be denied that a certain proportion of patients still cannot benefit from it, resulting in unsatisfactory prognosis expectations.[23] Consistent with the results of previous studies, this study found that among the 342 patients with ES-SCLC included, 13.2% of them still did not show a significant response to the chemoimmunotherapy regimen, which was also emphasized in the IMpower 133 and CASPIAN clinical trials mentioned earlier.[24,25] In view of this, seeking an early, convenient, and inexpensive chemoimmunotherapy response prediction and evaluation model is of great significance for screening patients with treatment response and avoiding delaying the treatment timing of non responsive patients. To the best of our knowledge, this is the first ES-SCLC chemoimmunotherapy response early warning, recognition, and prediction model constructed using radiomics and pathological section imaging. Although it is a preliminary exploration, the outcome is encouraging because the first treatment response prediction model constructed by combining multiple omics can identify patients sensitive to chemoimmunotherapy therapy before medication, which is the shared vision of clinical medical staff and patients.

The ideal biomarker not only needs to have the characteristics of convenience, affordability, practicality, and high predictive power, but also needs to be accepted by patients and widely used on the clinical front line. For example, Zhao et al used a comprehensive clinical and radiomics model to predict the treatment outcomes of ES-SCLC patients receiving chemoimmunotherapy, with a C-index value of 0.634 for predictive efficacy, providing a convenient and low-cost prognostic model for patient management decision-making.[15] However, there is still great room for improvement in its predictive efficacy. Coincidentally, many scholars have proposed using transcriptomics and tumor burden to achieve molecular typing of ES-SCLC, in order to predict treatment response. However, it cannot be denied that molecular subtyping has traceability advantages and can reveal the essence of its therapeutic response from the perspectives of transcription and translation.[26,27] However, the heterogeneity inherent in tumors is inevitable, which has led to the inability of previous molecular markers to be widely promoted, especially the poor prediction accuracy caused by the heterogeneity of tumor patients. Indeed, due to the gap between reality and ideals, we have to turn our attention to other available omics fields in order to seek more robust markers for predicting ES-SCLC treatment response.

Radiomics features, which capture biological and pathophysiological information, have provided fast and accurate non-invasive biomarkers for diagnosing, prognosticating, monitoring treatment response, and evaluating tumor biology in those diagnosed with cancer.[28] Our integrated prediction model is more effective and reliable in identifying patients benefitting from this treatment, thereby better guiding clinical diagnosis and treatment decisions. Previous studies have shown that traditional CT morphological features identify mutation burdens in malignant tumors (including EGFR mutations and ALK rearrangements in patients with SCLC). However, no studies have investigated the association between gene mutations and radiomics features in patients with ES-SCLC.[29–32] A preliminary exploration was conducted to address this gap. Consistent with previous research, CT texture analysis was used to distinguish imaging feature

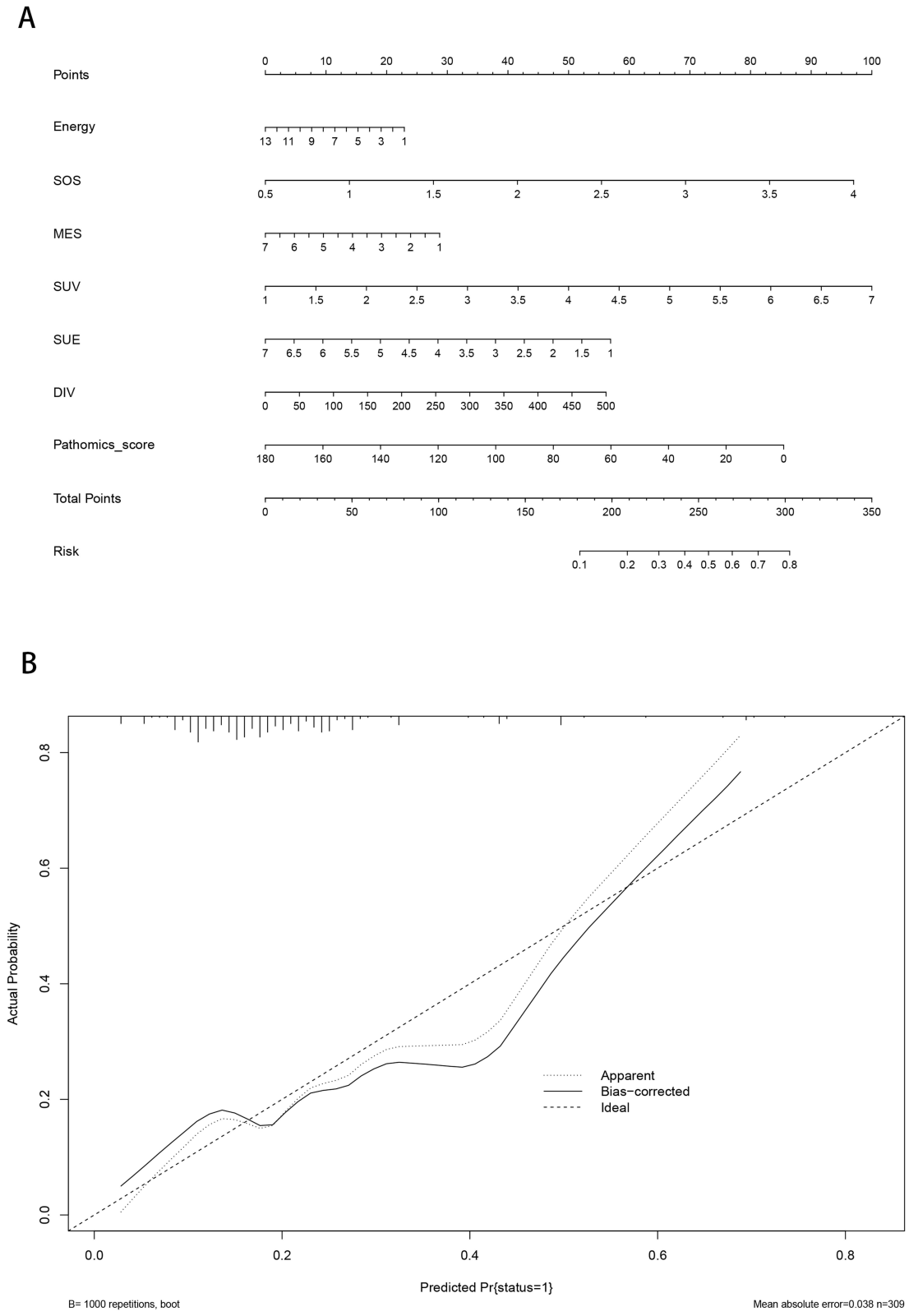

Figure 3 Nomogram for predicting ES-SCLC treatment response. (**A**) A nomogram chart, as each variable is assigned a value, where the radiomics and pathology of each patient are considered as dependent variables for evaluating treatment response, and a comprehensive score is obtained based on the assigned value. The corresponding risk value is the probability value of treatment response being "reactive" or "non- reactive"; (**B**) Calibration curve. By resampling the dataset 1000 times, the sample size of each sampling is included in the prediction model for evaluation, such as the calibration curve accompanying the diagonal, and the fit with the diagonal reflects the robustness of the prediction model.

Table 3 Evaluating the Predictive Ability of Four Machine Learning Prediction Models Based on the Area Under the ROC Curve

Prediction Model	Training Set				Testing Set			
	AUC	95% CI	PPV	NPV	AUC	95% CI	PPV	NPV
RFM	0.899	0.844~0.954	90.32	99.06	0.901	0.846~0.956	83.33	98.93
GLRM	0.764	0.707~0.821	82.76	97.20	0.792	0.735~0.849	66.67	96.77
DTM	0.801	0.744~0.858	68.97	95.33	0.794	0.737~0.851	53.85	95.65
ANNM	0.863	0.808~0.918	58.06	94.34	0.873	0.818~0.928	37.50	94.38

Abbreviations: AUC, Area under the curve; 95% CI, 95% confidence interval; PPV, Positive predictive value; NPV, negative predictive value; RFM, Random forest model; GLRM, Generalized linear regression model; DTM, decision tree; ANNM, artificial neural network model.

differences between responsive and non-responsive lesions to chemoimmunotherapy. Biomarkers for predicting treatment response were screened and selected by analyzing CT texture features (especially the distribution and relationship of pixel or voxel grayscale levels).[33,34] This study identified contrast, correlation, energy, diversity, entropy, homogeneity, and variance as independent risk factors for immune combined chemotherapy response. Significant differences in these radiomics characteristics were observed between responders and non-responders. It is hypothesized that the extracted texture features are interpretable, especially since texture analysis could reveal the heterogeneity of drug resistance in tumor lesions. Therefore, texture analysis is a potential biomarker for predicting drug resistance or response to immunotherapy combined with chemotherapy.

As is well known, pathological images embed basic prognostic data.[35] With the rise of full slide scanning technology, a large number of tissue slides are being digitally scanned, represented, and archived. It is worth mentioning that pathology is the integration of digital pathology and artificial intelligence, which is currently changing the landscape of medical pathology and biological disease classification. Previously, there have been emerging studies reporting the use of electronic pathology images to transform into pathological omics, in order to achieve diagnosis, treatment, and prognosis prediction of diseases.[36–38] However, it is still unknown whether key information on the volume changes of lesions after ES-SCLC combination therapy, especially in patients receiving combination therapy, can be obtained from pathological histology. In this study, we found that a deep learning model based on the addition of pathology can effectively predict treatment outcomes from histopathological images of tissues and can be transferred to new patient cohorts. Through the association with pathology, radiomics, and treatment response, although it is a retrospective study, the interpretability of our model lays the foundation for the prospective clinical trial of the application of this artificial intelligence platform in ES-SCLC treatment, especially the unparalleled performance of combined multi omics prediction of combined treatment response.

Using LASSO regression, this study screened seven widely used radiomics features and constructed an interpretable machine learning prediction model for chemoimmunotherapy response. Based on advanced machine learning algorithms, this model achieved high accuracy in predicting the risk stratification of patients receiving targeted therapy, significantly outperforming results reported in other studies.[39] It offers technical support for addressing targeted drug resistance in patients with ES-SCLC. Notably, even with the same radiomics parameters, the performance of predictive models varies significantly. Traditional generalized linear models derive independent risk factors through classic logical algorithms and construct risk prediction models using visual column charts. While these models provide valuable guidance for clinical diagnosis and treatment, they have drawbacks such as multicollinearity and overfitting compared to advanced algorithms like random forests and artificial neural networks.[40,41] Advanced algorithms, such as random forests, enhance the accuracy of prediction models without requiring extensive parameter inputs or significant medical investment, thereby optimizing prediction efficiency. This approach can reduce medical expenses and the economic burden on patients. Moreover, the visual prediction model based on random forests is interpretable, allowing clinicians to visualize each patient's prediction process, evaluate risk factors more clearly, and implement personalized decision-making assistance for targeted therapies.

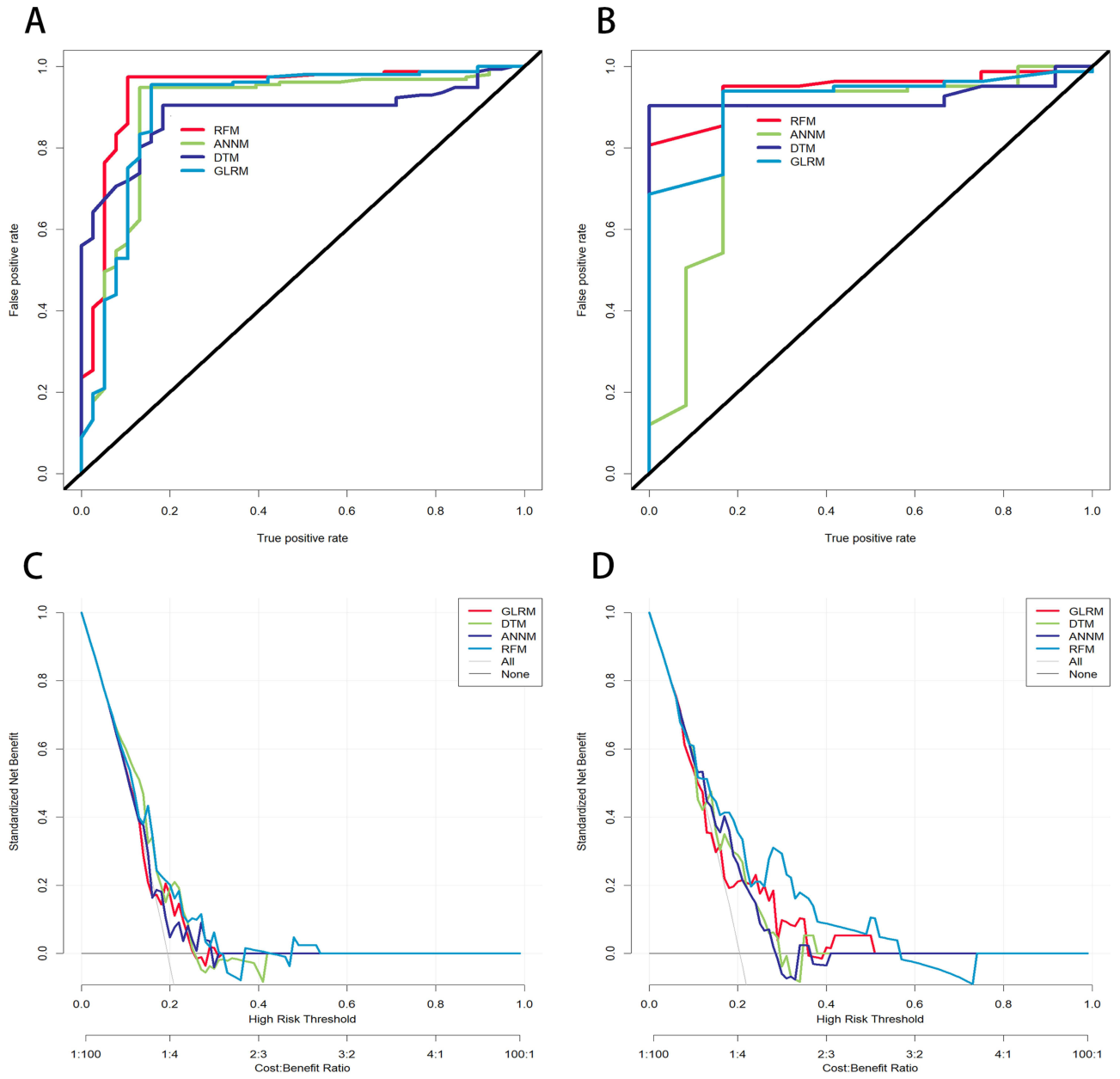

Figure 4 Evaluation of predictive performance of machine learning prediction models. Evaluate the predictive performance (ie area under the curve) of the prediction model based on ROC in the training set (**A**) and validation set (**B**); Evaluate the predictive performance (ie net benefit value) of the prediction model in the training set (**C**) and validation set (**D**) based on DCA.

This study inevitably has the following limitations. Firstly, despite achieving high efficiency in predicting the response of ES-SCLC to immunotherapy combined with chemotherapy, it is a retrospective study that poses the risk of variability in the CT scanner and acquisition parameters. Future research should standardize chest CT image acquisition and reconstruction to improve the reproducibility and generalizability of radiomics features. Secondly, as a single-center cohort study, it lacks the breadth of a large-sample, multicenter cohort. Therefore, it is necessary to collect diverse population cohort samples and conduct high-level prospective clinical trials to validate the practicality of radiomics, ensuring its repeatability and interpretability. Thirdly, while this study established a robust random forest prediction model using radiomics parameters, molecular imaging and clinical pathological parameters were not integrated. Multi-parameter fusion prediction models potentially improve prediction accuracy, warranting further exploration in future clinical decision support research.

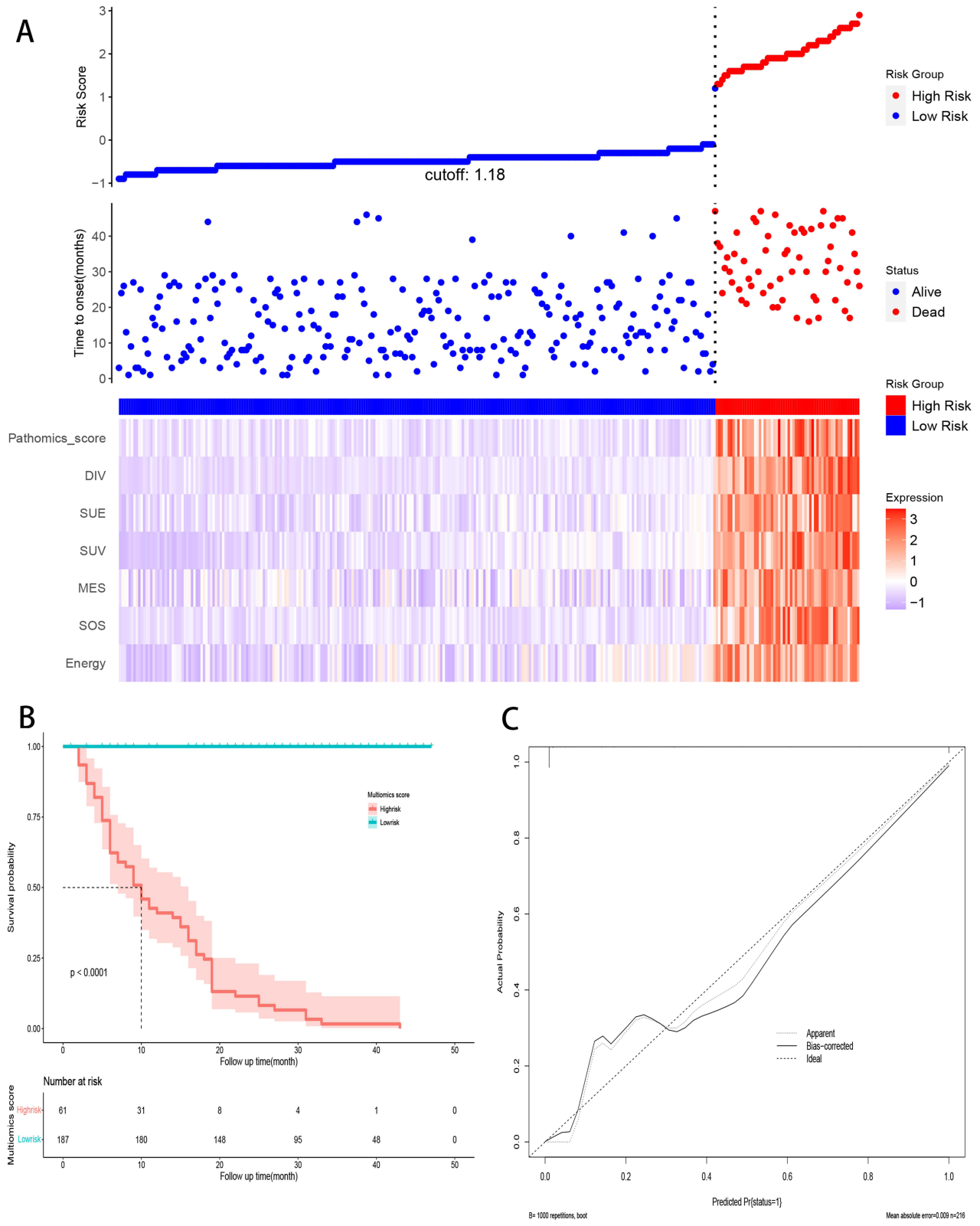

Figure 5 Prediction of OS after combined treatment based on radiation and pathology omics. (**A**)Risk factor diagram of the combined model in predicting OS; (**B**) K-M curves of OS by truncated value risk of predictive models; (**C**)The calibration curve of the combined prediction model at 6 months in predicting OS.

https://doi.org/10.2147/IJGM.S506485

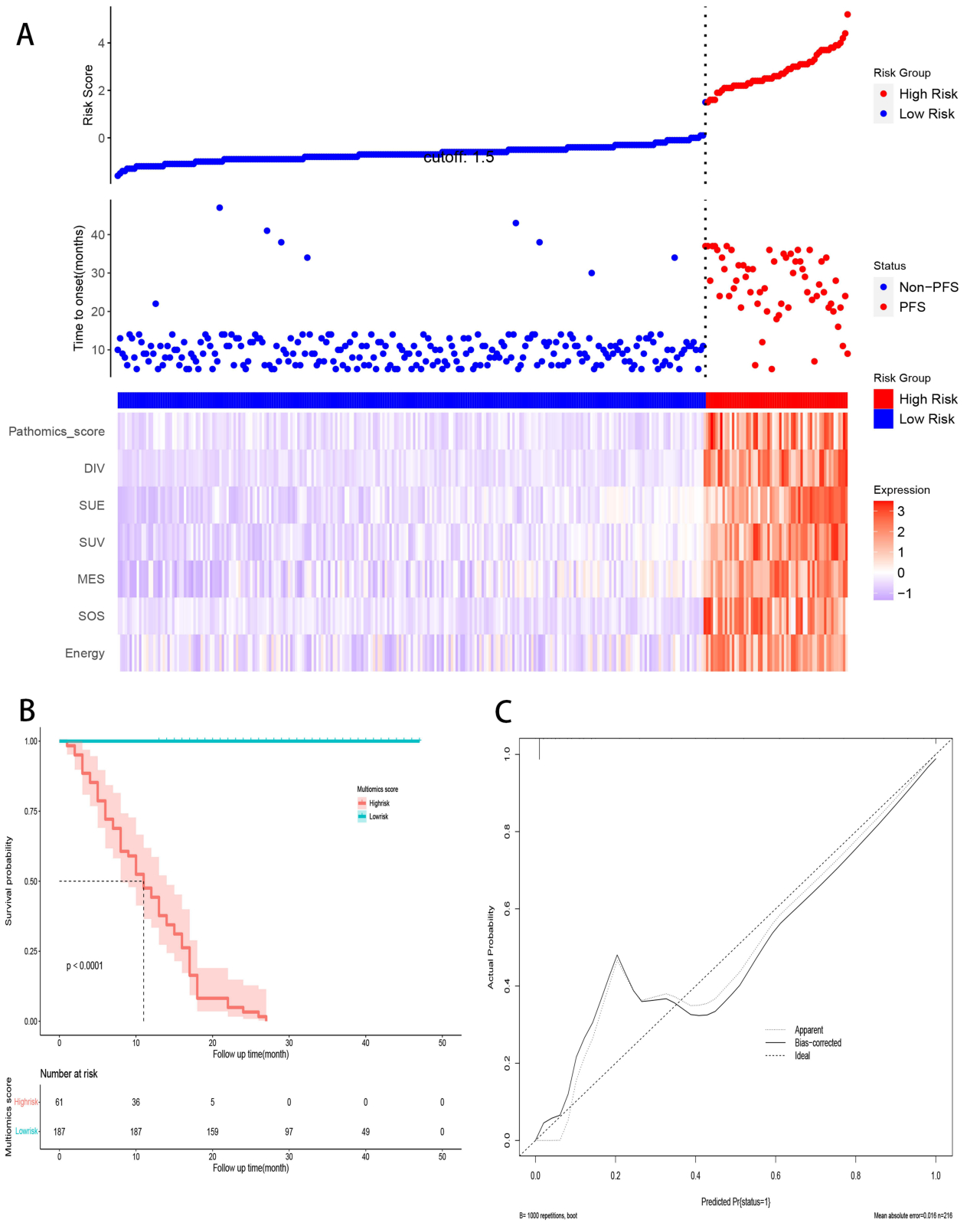

Figure 6 Prediction of PFS after combined treatment based on radiation and pathology omics. (**A**)Risk factor diagram of the combined model in predicting PFS; (**B**) K-M curves of PFS by truncated value risk of predictive models; (**C**)The calibration curve of the combined prediction model at 6 months in predicting PFS.

Conclusion

In summary, our prediction model for the response to immune combination chemotherapy, based on radiomics, pathological omics and machine learning algorithms, serves as a prognostic evaluation tool for predicting prognosis and treatment outcomes. This estimation assists in developing appropriate diagnostic and treatment plans, and follow-up strategies while effectively predicting patient prognosis.

Funding

1. Medical Research Development Fund Project Clinical and Basic Research Special Project (TB212008). 2. Beijing Cancer Prevention and Treatment Research Association (CAPTRALung2020005).

Disclosure

The authors report no conflicts of interest in this work.

References

1. Lee JH, Saxena A, Giaccone G. Advancements in small cell lung cancer. *Sem Cancer Biol*. 2023;93:123–128. doi:10.1016/j.semcancer.2023.05.008
2. Chauhan AF, Liu SV. Small cell lung cancer: advances in diagnosis and management. *Sem Respir Critical Care Med*. 2020;41(3):435–446. doi:10.1055/s-0039-1700566
3. Liang J, Guan X, Bao G, Yao Y, Zhong X. Molecular subtyping of small cell lung cancer. *Sem Cancer Biol*. 2022;86(Pt 2):450–462. doi:10.1016/j.semcancer.2022.05.010
4. Dingemans AC, Früh M, Ardizzoni A, et al. Small-cell lung cancer: ESMO Clinical Practice Guidelines for diagnosis, treatment and follow-up(☆). *Ann Oncol*. 2021;32(7):839–853. doi:10.1016/j.annonc.2021.03.207
5. Chu X, Han C, Su C. Treatment of small cell lung cancer: recent advances. *Current Opinion in Oncology*. 2022;34(1):83–88. doi:10.1097/CCO.0000000000000804
6. Canova S, Trevisan B, Abbate MI, et al. Novel therapeutic options for small cell lung cancer. *Curr Oncol Rep*. 2023;25(11):1277–1294. doi:10.1007/s11912-023-01465-7
7. Tian Y, Ma J, Jing X, et al. Radiation therapy for extensive-stage small-cell lung cancer in the era of immunotherapy. *Cancer Letters*. 2022;541:215719. doi:10.1016/j.canlet.2022.215719
8. Liu SV, Reck M, Mansfield AS, et al. Updated overall survival and PD-L1 subgroup analysis of patients with extensive-stage small-cell lung cancer treated with atezolizumab, carboplatin, and etoposide (IMpower133). *J Clin Oncol*. 2021;39(6):619–630. doi:10.1200/JCO.20.01055
9. Xie M, Vuko M, Rodriguez-Canales J, et al. Molecular classification and biomarkers of outcome with immunotherapy in extensive-stage small-cell lung cancer: analyses of the CASPIAN Phase 3 study. *Mol Cancer*. 2024;23(1):115. doi:10.1186/s12943-024-02014-x
10. Zugazagoitia J, Paz-Ares L. Extensive-stage small-cell lung cancer: first-line and second-line treatment options. *J Clin Oncol*. 2022;40(6):671–680. doi:10.1200/JCO.21.01881
11. Ragavan M, Das M. Systemic therapy of extensive stage small cell lung cancer in the era of immunotherapy. *Curr Treat Options Oncol*. 2020;21(8):64. doi:10.1007/s11864-020-00762-8
12. Petty WJ, Paz-Ares L. Emerging strategies for the treatment of small cell lung cancer: a review. *JAMA Oncol*. 2023;9(3):419–429. doi:10.1001/jamaoncol.2022.5631
13. Zhang S, Cheng Y. Immunotherapy for extensive-stage small-cell lung cancer: current landscape and future perspectives. *Front Oncol*. 2023;13:1142081. doi:10.3389/fonc.2023.1142081
14. Haug CJ, Drazen JM. Artificial intelligence and machine learning in clinical medicine, 2023. *New Engl J Med*. 2023;388(13):1201–1208. doi:10.1056/NEJMra2302038
15. Zhao J, He Y, Yang X, et al. Assessing treatment outcomes of chemoimmunotherapy in extensive-stage small cell lung cancer: an integrated clinical and radiomics approach. *J Immunother Cancer*. 2023;11(9):e007492. doi:10.1136/jitc-2023-007492
16. Caie PD, Harrison DJ. Next-Generation Pathology. *Methods Mol Biol*. 2016;1386:61–72.
17. Cui M, Zhang DY. Artificial intelligence and computational pathology. *Lab Invest*. 2021;101(4):412–422. doi:10.1038/s41374-020-00514-0
18. Eisenhauer EA, Therasse P, Bogaerts J, et al. New response evaluation criteria in solid tumours: revised RECIST guideline (version 1.1). *Eur J Cancer*. 2009;45(2):228–247. doi:10.1016/j.ejca.2008.10.026
19. Alhamzawi R, Ali HTM. The Bayesian adaptive lasso regression. *Math Biosci*. 2018;303:75–82. doi:10.1016/j.mbs.2018.06.004
20. van Egmond MB, Spini G, Van der Galien O, et al. Privacy-preserving dataset combination and Lasso regression for healthcare predictions. *BMC Med Inf Decision Making*. 2021;21(1):266. doi:10.1186/s12911-021-01582-y
21. Choi RY, Coyner AS, Kalpathy-Cramer J, Chiang MF, Campbell JP. Introduction to machine learning, neural networks, and deep learning. *Transl Vision Sci Technol*. 2020;9(2):14.
22. Deo RC. Machine Learning in Medicine. *Circulation*. 2015;132(20):1920–1930. doi:10.1161/CIRCULATIONAHA.115.001593
23. Sathiyapalan A, Febbraro M, Pond GR, Ellis PM. Chemo-immunotherapy in first line Extensive Stage Small Cell Lung Cancer (ES-SCLC): a systematic review and meta-analysis. *Curr Oncol*. 2022;29(12):9046–9065. doi:10.3390/curroncol29120709
24. Liu Q, Luo X, Yi L, Zeng X, Tan C. First-line chemo-immunotherapy for extensive-stage small-cell Lung cancer: a United States-based cost-effectiveness analysis. *Front Oncol*. 2021;11:699781. doi:10.3389/fonc.2021.699781
25. Landre T, Chouahnia K, Des Guetz G, Duchemann B, Assié JB, Chouaïd C. First-line immune-checkpoint inhibitor plus chemotherapy versus chemotherapy alone for extensive-stage small-cell lung cancer: a meta-analysis. *Therap Adv Med Oncol*. 2020;12:1758835920977137. doi:10.1177/1758835920977137

26. Yu Y, Chen K, Fan Y. Extensive-stage small-cell lung cancer: current management and future directions. *Int J Cancer*. 2023;152(11):2243–2256. doi:10.1002/ijc.34346
27. Liu SV, Mok TSK, Nabet BY, et al. Clinical and molecular characterization of long-term survivors with extensive-stage small cell lung cancer treated with first-line atezolizumab plus carboplatin and etoposide. *Lung Cancer*. 2023;186:107418. doi:10.1016/j.lungcan.2023.107418
28. Chen M, Copley SJ, Viola P, Lu H, Aboagye EO. Radiomics and artificial intelligence for precision medicine in lung cancer treatment. *Sem Cancer Biol*. 2023;93:97–113. doi:10.1016/j.semcancer.2023.05.004
29. de Margerie-Mellon C, Chassagnon G. Artificial intelligence: a critical review of applications for lung nodule and lung cancer. *Diagn Intervent Imaging*. 2023;104(1):11–17. doi:10.1016/j.diii.2022.11.007
30. Tong H, Sun J, Fang J, et al. A machine learning model based on PET/CT radiomics and clinical characteristics predicts tumor immune profiles in non-small cell lung cancer: a Retrospective Multicohort Study. *Front Immunol*. 2022;13:859323. doi:10.3389/fimmu.2022.859323
31. Avanzo M, Stancanello J, Pirrone G, Sartor G. Radiomics and deep learning in lung cancer. *Strahlentherapie und Onkologie*. 2020;196 (10):879–887. doi:10.1007/s00066-020-01625-9
32. Agazzi GM, Ravanelli M, Roca E, et al. CT texture analysis for prediction of EGFR mutational status and ALK rearrangement in patients with non-small cell lung cancer. *La Radiologia medica*. 2021;126(6):786–794. doi:10.1007/s11547-020-01323-7
33. Shen L, Fu H, Tao G, Liu X, Yuan Z, Ye X. Pre-immunotherapy contrast-enhanced CT texture-based classification: a useful approach to non-small cell lung cancer immunotherapy efficacy prediction. *Front Oncol*. 2021;11:591106. doi:10.3389/fonc.2021.591106
34. Mei D, Luo Y, Wang Y, Gong J. CT texture analysis of lung adenocarcinoma: can radiomic features be surrogate biomarkers for EGFR mutation statuses. *Cancer Imaging*. 2018;18(1):52. doi:10.1186/s40644-018-0184-2
35. Madabhushi A, Lee G. Image analysis and machine learning in digital pathology: challenges and opportunities. *Medical Image Analysis*. 2016;33:170–175. doi:10.1016/j.media.2016.06.037
36. Wu Y, Li Y, Xiong X, Liu X, Lin B, Xu B. Recent advances of pathomics in colorectal cancer diagnosis and prognosis. *Front Oncol*. 2023;13:1094869. doi:10.3389/fonc.2023.1094869
37. Schuettfort VM, Pradere B, Rink M, Comperat E, Shariat SF. Pathomics in urology. *Curr Opin Urol*. 2020;30(6):823–831. doi:10.1097/MOU.0000000000000813
38. Pan Y, Lei X, Zhang Y. Association predictions of genomics, proteinomics, transcriptomics, microbiome, metabolomics, pathomics, radiomics, drug, symptoms, environment factor, and disease networks: a comprehensive approach. *Med Res Rev*. 2022;42(1):441–461. doi:10.1002/med.21847
39. Swanson K, Wu E, Zhang A, Alizadeh AA, Zou J. From patterns to patients: advances in clinical machine learning for cancer diagnosis, prognosis, and treatment. *Cell*. 2023;186(8):1772–1791. doi:10.1016/j.cell.2023.01.035
40. Kernbach JM, Staartjes VE. Foundations of machine learning-based clinical prediction modeling: part II-generalization and overfitting. *Acta Neurochirurgica Supplement*. 2022;134:15–21.
41. Charilaou P, Battat R. Machine learning models and over-fitting considerations. *World J Gastroenterol*. 2022;28(5):605–607. doi:10.3748/wjg.v28.i5.605